Research Article

Journal of PeptideScience

Received: 4 April 2015 Revised: 24 May 2015 Accepted: 27 May 2015 Published online in Wiley Online Library: 7 July 2015

(wileyonlinelibrary.com) DOI 10.1002/psc.2795

Complementary DNA display selection of high-affinity peptides binding the vacuolating toxin (VacA) of *Helicobacter pylori*

**Yumiko Hayakawa,[a†] Mitsuhiro Matsuno,[a†] Makoto Tanaka,[a] Akihiro Wada,[b] Koichiro Kitamura,[c] Osamu Takei,[d] Ryuzo Sasaki,[a] Tamio Mizukami[a] and Makoto Hasegawa[a]*

Artificial peptides designed for molecular recognition of a bacterial toxin have been developed. Vacuolating cytotoxin A protein (VacA) is a major virulence factor of *Helicobacter pylori*, a gram-negative microaerophilic bacterium inhabiting the upper gastrointestinal tract, particularly the stomach. This study attempted to identify specific peptide sequences with high affinity for VacA using systematic directed evolution *in vitro*, a cDNA display method. A surface plasmon resonance-based biosensor and fluorescence correlation spectroscopy to examine binding of peptides with VacA identified a peptide (GRVNQRL) with high affinity. Cyclization of the peptide by attaching cysteine residues to both termini improved its binding affinity to VacA, with a dissociation constant (K_d) of 58 nM. This study describes a new strategy for the development of artificial functional peptides, which are promising materials in biochemical analyses and medical applications. Copyright © 2015 European Peptide Society and John Wiley & Sons, Ltd.

Keywords: artificial functional peptide; cDNA display method; *Helicobacter pylori*; *in vitro* peptide evolution; vacuolating cytotoxin A

Introduction

Artificial peptides recognizing particular molecules have several advantages over native antibodies, including greater thermal stability, reduced immunogenicity, and lower production costs using good manufacturing practice conditions. These peptides can be selected from random sequence libraries by display methods (genotype–phenotype linkage technology) including phage display [1,2], ribosome [3,4], mRNA, and cDNA [5–9] methods. These techniques usually involve evolutionary molecular screening via three steps: (i) a synthetic (composites) step linking phenotypic peptides to genotypic polynucleotides, (ii) a selection step for the peptide–polynucleotide composites involving affinity-based selection for a target molecule, and (iii) an amplification step involving the selected peptide–polynucleotide composites. Iteration through several cycles of these steps is required to converge sufficiently on a peptide sequence with high affinity for the target molecule. To date, these display methods have generated many peptides that specifically interact with target proteins, such as proteases [9], kinases, transcription factors [10], signaling regulators, receptors [11–14], and viral proteins [15,16]. Thus, the selected peptides are ideal candidates for molecular recognition elements in biochemical analyses, owing to their specificity, high-binding affinity, stability, easy preparation, and ability to be conjugated to a variety of chemical moieties.

The cDNA display method [8,9,11–14] is an improved version of the mRNA display method [5–7], avoiding the instability of mRNA. Peptide-RNA covalent composites are formed using a well-designed puromycin linker. Stable peptide-RNA/DNA composites are generated by continuous processes of mRNA transcription, cell-free translation, and reverse transcription (Fig. 1) [17,18]. All of the steps in cDNA display are performed *in vitro* to overcome library size limitation, a drawback of the phage display method that requires transformation of bacteria. Peptide-RNA/DNA composites are screened using affinity beads on which the target molecule has been immobilized. The selected composites are amplified by polymerase chain reaction for the next cycle. Five to eight repetitive cycles enable identification of converged sequences of peptides that bind specifically to the target molecule.

Bacterial toxins disturb host biological processes, resulting in cellular damage. Specific antibodies play important roles in the diagnosis, treatment, and prevention of bacterial toxin virulence. Attempts have been made to develop artificial peptides for targeting bacterial toxins [19–25]. Vacuolating cytotoxin A (VacA) is produced by *Helicobacter pylori*, infection with which frequently

* *Correspondence to: Makoto Hasegawa, Graduate School of Bioscience, Nagahama Institute of Bio-Science and Technology, Tamura 1266, Nagahama, Shiga 526-0829, Japan. E-mail: m_hasegawa@nagahama-i-bio.ac.jp*

† *These authors contributed equally to this work.*

a *Graduate School of Bioscience, Nagahama Institute of Bio-Science and Technology, Tamura 1266, Nagahama, Shiga 526-0829, Japan*

b *Institute for Tropical Medicine, Nagasaki University, Sakamoto 1-12-4, Nagasaki 852-8523, Japan*

c *JANUSYS Co., Ltd., Kamiaoki 3-12-18-508, Kawaguchi, Saitama 333-0844, Japan*

d *Lifetech Co., Ltd., Miyadera 4074, Iruma, Saitama 358-0014, Japan*

Journal of PeptideScience

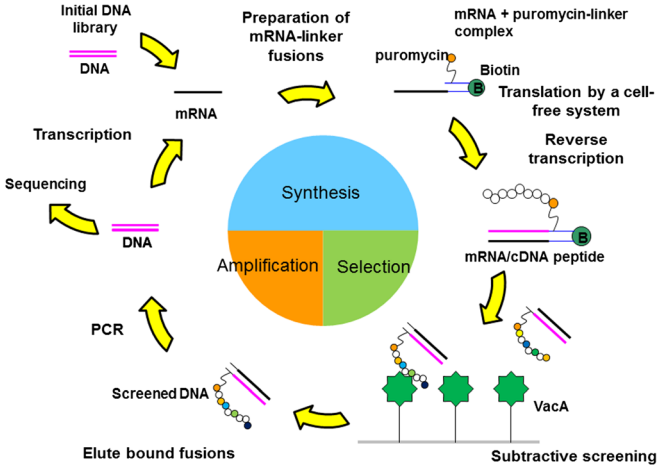

Figure 1. Schematic representation of the *in vitro* selection of VacA-binding peptides.

causes chronic gastritis, peptic ulcers, and stomach cancer [26]. VacA induces multiple detrimental effects on epithelial and lymphatic cells, including alterations of endo-lysosomal function, anion-selective channel formation, and mitochondrial function [27]. The toxin VacA is a large protein complex (~1000 kDa), composed of more than seven VacA molecules, and forming ring structures.

In this study, VacA-binding peptides with high affinity and specificity were generated using cDNA display screening. Molecular interaction analyses with fluorescence correlation spectroscopy showed that these peptides induced marked aggregation of VacA. Interaction of these peptides with VacA was chemically demonstrated by using photoreactive peptide derivatives that could link to VacA. Interestingly, cyclic peptides showed higher affinity than the original linear forms, suggesting that cyclic peptides may be a minimum scaffold required for high-affinity binding to VacA. The properties of these peptides suggest that they may be beneficial in detecting the toxin.

Materials and Methods

cDNA Display Method

VacA-binding peptide candidates were obtained using a cDNA display method as described [14,28] (Fig. 1). This study used a cDNA display library encoding random eight-amino acid peptides [9]. VacA, prepared as described [29], was immobilized on NHS-activated Sepharose beads (GE Healthcare Japan Co., Tokyo, Japan) using amine coupling chemicals to form a chemically stable amide bond in accordance with the manufacturer's instructions.

The cDNA display library was diluted in 100 µl of selection buffer (0.1 M NaCl in PBST, pH 7.4) and incubated with 10 µl of VacA-immobilized beads, containing about 10 pmol VacA. The beads were washed with 200 µl of selection buffer, washing buffer 1 (0.25 M NaCl in PBST, pH 7.4), washing buffer 2 (0.5 M NaCl in PBST, pH 7.4), washing buffer 3 (1 M NaCl in PBST, pH 7.4), and washing buffer 4 (2 M NaCl in PBST, pH 7.4). Each round of washing utilized different conditions to gradually enhance the selection pressure (Table 1). After washing, the beads were suspended in 100 µl of elution buffer 1 (2 M NaCl and 10 mM $MgCl_2$ in PBST, pH 7.4) and incubated at 37 °C for 5 min, and the supernatant was collected (Sup1). The beads were suspended in 100 µl elution buffer 2 (4 M NaCl and 10 mM $MgCl_2$ in PBST, pH 7.4) and incubated at 95 °C for 5 min, and the supernatant was collected (Sup2). Sup1 and Sup2 were purified by ethanol precipitation. The cDNA portion of the purified sample was amplified using polymerase chain reaction for the next round of selection or cloned into TOPO® TA Cloning® Kits with pCR®2.1-TOPO vector (Thermo Fisher Scientific, Inc., MA, USA) and used for sequencing.

Peptide Synthesis

Peptides were synthesized by standard Fmoc/HBTU chemistry. Synthetic peptides were extended by stepwise coupling on a Wang resin carrying an Fmoc-protected amino acid (Watanabe Chemical Industries, Ltd., Hiroshima, Japan) on a 433A peptide synthesizer (Thermo Fisher Scientific, Inc.). The synthetic peptides were deprotected and cleaved from resin using a reagent containing trifluoroacetic acid (TFA) and scavenging agents as described in the synthesizer's manual. Crude peptides were purified with a high-performance liquid chromatography (HPLC) system (Gilson, Inc., WI, USA), equipped with a reverse phase column (COSMOSIL, $5C_{18}$-AR-II, 4.6 × 150 mm, Nacalai Tesque Inc., Kyoto, Japan). HPLC was performed at a flow rate of 1 ml/min with a linear gradient of 5–50% CH_3CN in 0.05% TFA in water. Peptide purities were confirmed using a Spiral-TOF JMS-S3000 mass spectrometer (JEOL Ltd., Tokyo, Japan).

Chemical Modification of Peptides

Peptides were labeled with BODIPY® FL (Thermo Fisher Scientific, Inc.), biotin-AC_5-OSu (Dojindo Laboratories Co. Ltd., Kumamoto,

Table 1. Selection conditions for each round

Round	Incubation temperature and time	Numbers of washes				
		Selection buffer	Wash buffer 1	Wash buffer 2	Wash buffer 3	Wash buffer 4
1	25 °C, 15 min	3	3	—	—	—
2	25 °C, 15 min	—	3	2	—	—
3	25 °C, 15 min	—	2	3	1	—
4	37 °C, 5 min	—	1	3	2	—
5	37 °C, 5 min	—	—	2	3	—
6	25 °C, 15 min	3	—	—	3	—
7	25 °C, 15 min	—	—	—	3	3*
8	37 °C, 5 min	—	—	—	—	6†

* 2, 3rd, +25 °C, 15 min incubation.
† 4–6th, +37 °C, 15 min incubation.

Japan), or sulfo-SBED (sulfo-N-hydroxysuccinimidyl-2-(6-[biotinamido]-2-(*p*-azidobenzamido)-hexanoamido)-ethyl-1,3′-dithioproprionate, Thermo Fisher Scientific, Inc.). The peptides modified by sulfo-SBED were termed BAED peptides. In each reaction, a peptide was esterified with an equimolar reagent in dimethylformamide containing 100 equivalents of triethylamine. After incubating for 6–12 h at room temperature, each product was purified by reverse phase HPLC as described previously. Combinations of tryptic digestion and tandem mass spectrometry (MS/MS) measurements (data not shown) were used to confirm the selective reaction of a chemical moiety with the N-terminal amino group.

Surface Plasmon Resonance (SPR) Biosensor Measurements

For SPR-biosensor measurements, sensor chips consisting of gold slides were prepared for immobilization using each biotinylated peptide. Prior to use, the sensor chip surface was cleaned in piranha solution (H_2SO_4:H_2O_2, 7:3, v/v) for 5 min and rinsed several times with deionized water. Sensor chips were immediately immersed in a 1 mM chloroform solution containing 11-hydroxy-1-undecanethiol/HS-$(CH_2)_{11}$-NH-C(O)-biotin (9 :1) to generate self-assembled monolayers and were incubated overnight at room temperature. On removal from the chloroform solution, the slides were sequentially rinsed with chloroform, followed by drying in a stream of N_2 gas.

Each biotinylated peptide was fixed on the sensor chip surface through tetrameric streptavidin, which functioned as a linker between the peptide and the self-assembled monolayer. An SPR-M1 biosensor system (Optoquest Co. Ltd., Saitama, Japan) was used to measure SPR shifts. As the amounts of immobilized streptavidin differed among individual experiments, each resonance unit (RU) was normalized by the ΔRU of the corresponding streptavidin treatment. In evaluating each immobilized peptide, 1 μM of VacA solution was injected into the SPR biosensor. RU responses reaching a plateau were regarded as the maximum binding capacity of the peptide on the sensor surface and were recorded.

Fluorescence Correlation Spectroscopy (FCS) Measurements

Fluorescence correlation spectroscopy measurements were performed using a commercial FCS setup, FCS-101B (Hamamatsu Photonics K. K., Hamamatsu, Japan). An excitation wavelength of $\lambda = 473$ nm was provided by a diode-pumped solid-state laser, and fluorescent light of $\lambda > 520$ nm was separated by a band path filter in front of the pinhole and detected by a photomultiplier.

Fluorescence correlation spectroscopy measurements of labeled peptides were performed in phosphate buffered saline (PBS). Various concentrations of the VacA solution and 10 nM of a labeled peptide were incubated with PBS containing 0.2 mg/ml of bovine serum albumin at 37 °C for 1 h. After incubation, samples were transferred onto a slide glass, and molecular diffusion times were measured in solution. For data analysis, the scans were averaged and plotted by a graphical analysis program supplied by the device manufacturer. The fitting routine was performed using this same data analysis program.

Photoaffinity Labeling

VacA (1 μg in a 50 μl reaction mixture) was incubated with the photoreactive biotinylated peptide, BAED-GRVNQRL (0.5 μM), in the presence or absence of the unmodified peptide GRVNQRL (10 μM). Bovine serum albumin (BSA) (1 μg in a 50 μl reaction mixture) was added to all reaction mixtures (50 mM Tris-HCl, pH 7.6, and 100 mM NaCl) to examine the specific labeling of VacA by the peptide. After incubation for 60 min at 37 °C, the reaction mixtures for binding of peptide to VacA were exposed to ultraviolet (UV) light (254 nm) for 40 min on ice. The proteins were separated by sodium dodecyl sulfate polyacrylamide gel electrophoresis (SDS-PAGE) and transferred and immobilized onto polyvinylidene difluoride membranes, which were incubated with horseradish peroxidase-conjugated streptavidin (GE Healthcare Japan Co.). Chemiluminescence images were obtained with a LAS-4000 (GE Healthcare Japan Co.). VacA and BSA bands were detected by Sypro-Red (Thermo Fisher Scientific, Inc.) staining, confirming that equal amounts of each protein were applied.

Results

Identification of VacA-Binding Peptides by *in Vitro* Evolutionary Selection

The composite peptide-mRNA/cDNA preparation theoretically contained more than one copy of random peptides, each consisting of eight amino acids, in the initial library [14,28]. After eight cycles (Fig. 1), 54 clones that might contain peptide sequences, which likely interacted with VacA, were sequenced. The resulting 30 peptides were chemically synthesized and biotinylated at their N-termini. Peptides that contained more than one cysteine residue were excluded because they might produce oligomeric complexes or unexpected intramolecular cyclized forms via disulfide bridges. VacA-binding of the 30 peptides was analyzed using an SPR biosensor equipped with each peptide-immobilized sensor chip. Responses in resonance units (ΔRU) after injection of 1 μM VacA are summarized in Fig. 2. Inspection of peptide sequences revealed that 13 peptides with robust binding to VacA had a consensus sequence of Gly-Arg-X_1-Asn/Thr-Gln/Ser-X_2-(X_3)-Leu/Ile (X_1: hydrophobic amino acids, Val, Leu, Tyr, and Trp; X_2: any amino acid; and (X_3): any amino acids or none) (Table 2). These peptides frequently contained Gly, Ser, Asn, and Tyr residues with the secondary structure-forming propensity in protein [30], suggesting that the presence of these residues facilitated the formation of β-turn structures. The other peptides were relatively

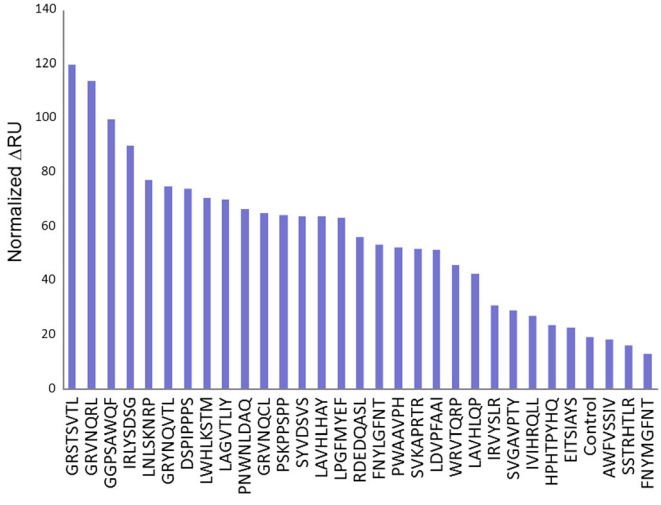

Figure 2. Binding of the peptide to VacA, as determined by measuring surface plasmon resonance (SPR). Peptides selected by the cDNA display method were biotinylated, with each immobilized on a streptavidin-treated sensor chip. The change in refractive index on the sensor surface after injection of 1 μM VacA solution was evaluated (ΔRU).

Journal of PeptideScience

Table 2. Peptides evaluated as high-affinity sequences by SPR sensor measurements.

Order	Sequence
1	**Gly-Arg**-Ser-**Thr-Ser**-Val-Thr-**Leu**
2	**Gly-Arg-Val-Asn-Gln**-Arg-**Leu**
3	**Gly**-Gly-Pro-Ser-Ala-Trp-**Gln**-Phe
4	Ile-**Arg-Leu**-Tyr-**Ser**-Asp-Ser-Gly
5	Leu-Asn-Leu-Ser-Lys-Asn-Arg-Pro
6	**Gly-Arg-Tyr-Asn-Gln**-Val-Thr-**Leu**
7	Asp-Ser-Pro-Ile-Pro-Pro-Pro-Ser
8	Leu-Trp-His-Leu-Lys-Ser-Thr-Met
9	Leu-Ala-Gly-Val-**Thr**-Leu-**Ile**-Tyr
10	Pro-Asn-**Trp**-Asn-Leu-Asp-Ala-Gln
11	**Gly-Arg-Val-Asn-Gln**-Cys-**Leu**
12	Pro-Ser-Lys-Pro-Pro-Ser-Pro-Pro
13	Ser-Tyr-**Val**-Asp-Ser-Val-Ser
Consensus sequence	Gly-Arg-X_1-Asn/Thr-Gln/Ser-X_2-(X_3)-Leu/Ile

X_1: hydrophobic amino acids, Val, Leu, Tyr, and Trp; X_2: any amino acid. (X_3): any amino acid or none. Bold characters indicate amino acid residues corresponding to the consensus sequence.

high in hydrophobic residues, but no consensus sequence was identified. Thus, further experiments focused on the 13 peptides with the previously mentioned consensus sequence.

Molecular Interaction Analysis by Fluorescence Correlation Spectroscopy Measurements

Interaction of a fluorescent-labeled peptide with VacA increases the apparent size of the bound peptide, thereby reducing its diffusion rate. Measurement of fluorescence fluctuations enables estimations of the change in size of the bound peptide and the dissociation constant (K_d) of the peptide-VacA complex. FCS analyses of the interaction of the BODIPY FL-labeled peptide (FL-GRVNQRL) with VacA showed that the diffusion time (τ) of the peptide was increased upon incubation with VacA (Fig. 3(A)). The τ of FL-GRVNQRL was not affected by the presence of other proteins, such as cholera toxin B subunit, casein, and bovine serum albumin, indicating that binding of this peptide to VacA is highly specific (data not shown). Interestingly, an increase in τ of fluorescent-labeled VacA (Alexa488-VacA) was observed upon incubation with non-labeled GRVNQRL (Fig. 3(B)), suggesting the peptide-induced aggregation of VacA.

Peptide cyclization is increasingly used in designing bioactive compounds [14,31–35]. Cyclization of a peptide apparently restricts its conformational flexibility, resulting in the generation of a peptide that has high affinity to the target molecule. To examine this effect, the cyclic form of GRVNQRL was prepared by adding cysteine residues to both termini, followed by subsequent intramolecular disulfide bridge formation, generating the fluorescent-labeled cyclic form, FL-CGRVNQRLC. FCS was utilized in kinetic analyses of the interactions of linear and cyclic peptides with varying concentrations of VacA. All autocorrelation data were analyzed by nonlinear regression to provide τ values for the bound and unbound peptides. The molecular ratio of VacA-bound to VacA-unbound peptide was evaluated by Scatchard plot analysis to determine the dissociation constants of the peptides. Cyclization of GRVNQRL increased its binding affinity; the K_d of the linear peptide for VacA was 213 nM, whereas the K_d of the cyclic peptide was 58 nM (Fig. 4). FCS analyses confirmed that the peptide FL-IRLYSDSG, which poorly matched with the consensus sequence (Table 2), had a weak affinity to VacA, although high concentrations showed significant binding to VacA.

Interaction-induced changes in the molecular sizes of peptide and VacA were estimated by FCS measurements using BODIPY FL-GRVNQRL or Alexa488-VacA (Table 3). The unbound FL-GRVNQRL exhibited a τ of 0.0437 ms, the intrinsic value corresponding to the molecular weight of the peptide (1.4 kDa). FL-GRVNQRL bound to VacA exhibited a τ of 1.14 ms, suggesting that a large complex of VacA (around 20 MDa) is formed upon interaction with FL-GRVNQRL. This finding was confirmed by FCS measurements using fluorescent Alexa488-labeled VacA. The τ value of VacA increased from 0.181 ms (100 kDa) in the absence of the peptide to 1.40 ms (50 MDa) following addition of 1 μM GRVNQRL. As the molecular mass of monomeric VacA is 87–95 kDa, the molecular mass (100 kDa) observed in the absence of the peptide likely represents the monomer state. Thus, peptide binding likely induces marked aggregation of VacA, resulting in a large complex consisting of several hundred VacA molecules. The molecular mechanism by which the peptide induces VacA aggregation remains to be determined. Oligomerization of VacA appears to be an intrinsic property closely associated with its toxicity [36]. The selected peptide may simply promote expression of this property.

Affinity Labeling of VacA Using a Photoreactive Peptide Derivative

The specific binding of selected peptides to VacA was chemically verified using an affinity-labeling technique, in which a photoreactive

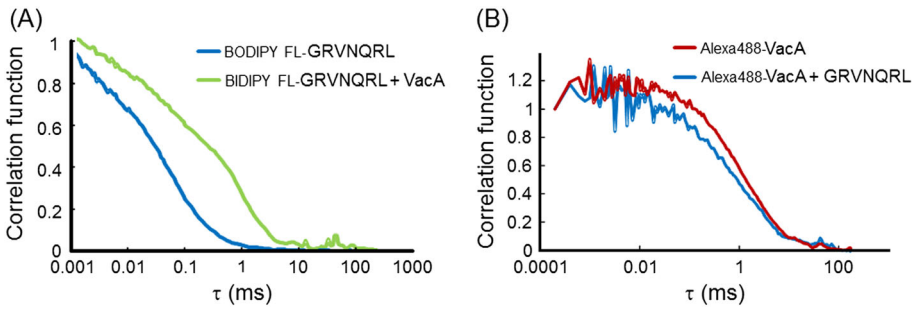

Figure 3. Fluorescence correlation spectrometry (FCS). FCS measurements were performed to detect fluorescence fluctuations generated upon interaction of the fluorescent peptide (BODIPY FL-GRVNQRL) with VacA or the fluorescent VacA (Alexa488-VacA) with the non-labeled peptide (GRVNQRL). Data of fluctuations were analyzed as described in Materials and Methods to estimate diffusion time (τ) of fluorescent materials. (A) shows autocorrelation curves when 10 nM fluorescent peptide was mixed with or without 1 μM VacA and (B) shows autocorrelation curves when 1 μM fluorescent VacA was mixed with or without 1 μM non-labeled peptide.

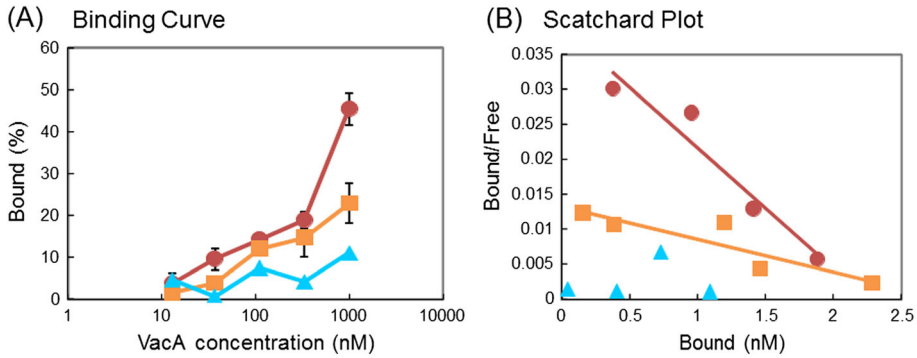

Figure 4. Kinetic analyses of binding of fluorescent-labeled peptides with VacA. Circularization of the peptide using an intramolecular disulfide bridge resulted in increased affinity. Fluorescent-labeled peptides (10 nM) were incubated with VacA at various concentrations, and peptide binding was evaluated by FCS. Binding curves (A) and Scatchard plot analyses (B) are of circular (●) and linear (■) peptides of GRVNQRL, and the linear peptide of IRLYSDSG (▲).

Table 3. Diffusion times (τ) and molecular weights evaluated by τ using Eqn (1). [41]

	Diffusion time (τ) (ms)	Molecular weight
BODIPY FL-GRVNQRL (10 nM)	0.0437	1.4×10^3
BODIPY FL-GRVNQRL (10 nM) + VacA (1 μM)	1.14	2.0×10^7
Alexa488-VacA (1 μM)	0.181	1.0×10^5
Alexa488-VacA (1 μM) + GRVNQRL (1 μM)	1.40	5.0×10^7

$$MW_{sample} = \left(\frac{\tau_{sample}}{\tau_{Alexa\ 488}}\right)^3 \times MW_{Alexa\ 488} \quad (1)$$

peptide containing a biotin group, BAED-GRVNQRL (Fig. 5(A)), was cross-linked to VacA. Following cross-linking and SDS-PAGE, the affinity-labeled VacA was detected as a chemiluminescence-emitting band upon UV irradiation. Binding of the photoreactive peptide to VacA was reduced in the presence of the unmodified peptide (Fig. 5(B)), confirming that the BAED group in the photoreactive peptide did not interfere with the interaction of the peptide with VacA. No chemiluminescent VacA was detected in the absence of UV irradiation. BSA was included in all reaction mixtures, but no chemiluminescent BSA was found, confirming that the peptide bound specifically to VacA. The loading of equal amounts of proteins on gels was confirmed by protein staining with Sypro-Red (Fig. 5(B), bottom panel).

Kinetic analyses of the interactions of a fluorescent peptide with VacA by FCS showed that cyclization of the peptide increased its affinity to VacA (Fig. 4). To examine whether this is also observed with other peptides, competitive binding assays were performed. In these assays, the binding of photoreactive BAED-GRVNQRL to VacA was examined in the presence or absence of other peptides and their cyclic forms. Whereas the addition of the linear peptides reduced labeled VacA bands to some degree, each cyclic peptide inhibited BAED-GRVNQRL binding to a greater extent than the corresponding linear peptide, confirming that cyclization of the peptide candidates increases their binding affinity to the target protein (Fig. 5(C)). These results indicate that peptide cyclization is useful in generating high-affinity peptides.

Discussion

In this study, artificial VacA-binding peptides were generated using a cDNA display method. These high-affinity peptides had a consensus sequence of Gly-Arg-X_1-Asn/Thr-Gln/Ser-X_2-(X_3)-Leu/Ile, in which X_1 represents hydrophobic amino acids such as Val, Leu, Tyr, and Trp; X_2 represents any amino acid; and (X_3) represents an additional inserted amino acid. Constraining the conformational flexibility of these linear peptides by attaching cysteine residues at both termini, followed by disulfide linking, markedly increased peptide binding affinity to VacA. The peptides induced marked aggregation of VacA. Although the molecular mechanism has not been determined, peptide-induced aggregation of VacA may sensitize medical diagnostic test kits such as those using latex coagulating methods.

cDNA display screening using a disulfide-rich peptide library was reported to generate an interleukin (IL)-6 antagonistic peptide with high affinity [12]. In that study, a 32 amino acid peptide was designed to form two disulfide bridges. Such screening should be effective for identifying high-affinity peptides of more than ten residues because plural disulfide linkages often provide biologically highly active structures, as seen in cysteine-rich toxic peptides such as conotoxins. The cyclized peptides used in this study were generated by adding cysteine residues at both termini selected during cDNA display. As spontaneous intramolecular cyclization proceeds by air oxidation, this method may be the easiest for improving the binding affinity of short linear peptides. The cyclic peptides naturally form a β-turn structure, which may be a minimum scaffold for binding to VacA with high affinity.

Efforts have been made to develop various scaffolds on which peptides can be immobilized, stabilizing their functional conformations. Engineered protein scaffolds, which often use rigid natural protein structures, including protein A [37], fibronectin [38], and ankyrin repeats [39,40], are promising materials for improving the binding properties of short antibody-like peptides generated by the RNA/cDNA display method. For example, a three-finger scaffold (MicTx3) was successfully used to obtain ligands of a target protein (IL-6R), with generated peptides inserted into the top regions of finger-like loop structures in the scaffold [11]. Repetitively branched synthetic molecules, dendrimers, are non-protein scaffolds with multivalent binding motifs. A small dendrimer carrying four peptides was shown to inhibit the virulence of Shiga toxin [22]. Application of dendrimers to VacA-binding peptides is currently

Journal of PeptideScience

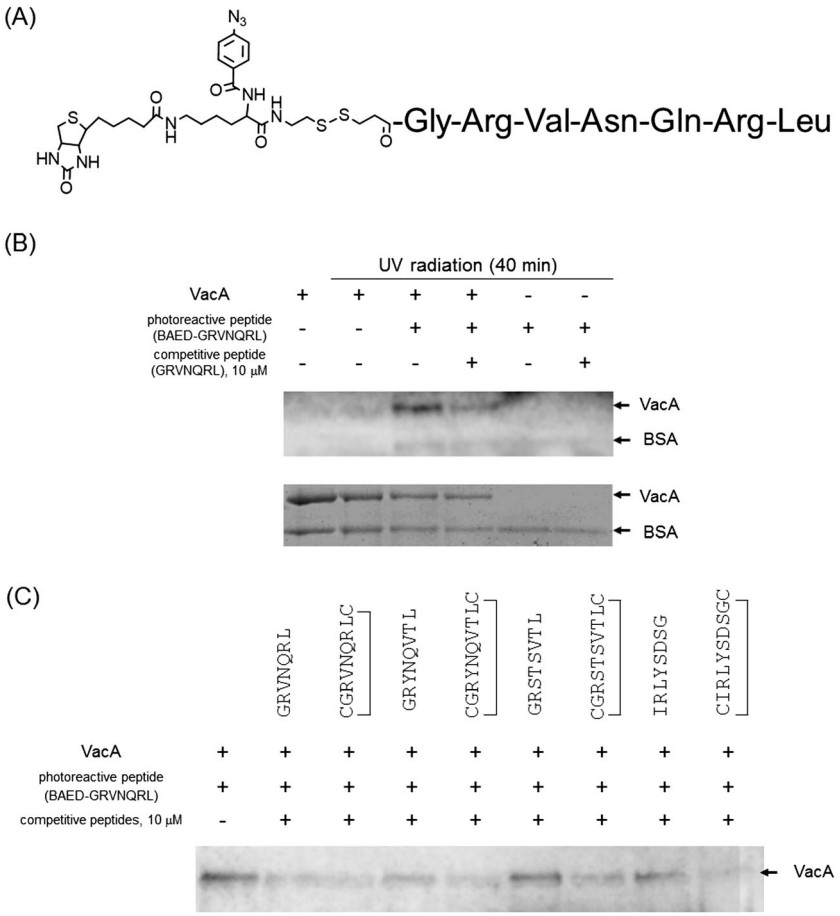

Figure 5. Binding of photoreactive biotinylated peptide to VacA and increased affinity upon circularization. (A) Structure of the photoreactive biotinylated peptide, BAED-GRVNQRL. (B) VacA (1 μg in a 50 μl reaction mixture) was incubated with the photoreactive biotinylated peptide, BAED-GRVNQRL (0.5 μM), in the presence or absence of the peptide competitor (10 μM) (see the top panel for detailed conditions). In middle panel, VacA carrying the biotinylated peptide was visualized by detecting the chemiluminescence emitted by peroxidase-conjugated streptavidin. In the bottom panel, VacA and BSA bands were detected by Sypro-Red staining, confirming that equal amounts of each protein were applied. (C) Labeling of VacA with the photoreactive biotinylated peptide, BAED-GRVNQRL, and detection of the labeled VacA as in (B). Linear peptides and their circularized counterparts (10 μM) shown in the top panel were added as competitors to the binding of peptide with VacA.

under investigation to determine whether the peptides generated here may be useful diagnostic and therapeutic agents.

References

1 Smith GP. Filamentous fusion phage: novel expression vectors that display cloned antigens on the virion surface. *Science.* 1985; **228**: 1315–1317.
2 Smith GP, Petrenko VA. Phage display. *Chem. Rev.* 1997; **97**: 391–410.
3 Hanes J, Plückthun A. *In vitro* selection and evolution of functional proteins by using ribosome display. *Proc. Natl. Acad. Sci. U S A.* 1997; **94**: 4937–4942.
4 Mattheakis LC, Bhatt RR, Dower WJ. An *in vitro* polysome display system for identifying ligands from very large peptide libraries. *Proc. Natl. Acad. Sci. U S A.* 1994; **91**: 9022–9026.
5 Roberts RW, Szostak JW. RNA-peptide fusions for the *in vitro* selection of peptides and proteins. *Proc. Natl. Acad. Sci. U S A.* 1997; **94**: 12297–12302.
6 Keefe AD, Szostak JW. Functional proteins from a random-sequence library. *Nature* 2001; **410**: 715–718.
7 Seelig B, Szostak JW. Selection and evolution of enzymes from a partially randomized non-catalytic scaffold. *Nature* 2007; **448**: 828–831.
8 Nemoto N, Miyamoto-Sato E, Husimi Y, Yanagawa H. *In vitro* virus: bonding of mRNA bearing puromycin at the 3′-terminal end to the C-terminal end of its encoded protein on the ribosome *in vitro*. *FEBS Lett.* 1997; **414**: 405–408.
9 Kitamura K, Yoshida C, Kinoshita Y, Kadowaki T, Takahashi Y, Tayama T, Kawakubo T, Naimuddin M, Salimullah M, Nemoto N, Hanada K, Husimi Y, Yamamoto K, Nishigaki K. Development of systemic *in vitro* evolution and its application to generation of peptide-aptamer-based inhibitors of cathepsin E. *J. Mol. Biol.* 2009; **387**: 1186–1198.
10 Nagel-Wolfrum K, Buerger C, Wittig I, Butz K, Hoppe-Seyler F, Groner B. The interaction of specific peptide aptamers with the DNA binding domain and the dimerization domain of the transcription factor Stat3 inhibits transactivation and induces apoptosis in tumor cells. *Mol. Cancer. Res.* 2004; **2**: 170–182.
11 Naimuddin M, Kobayashi S, Tsutsui C, Machida M, Nemoto N, Sakai T, Kubo T. Directed evolution of a three-finger neurotoxin by using cDNA display yields antagonists as well as agonists of interleukin-6 receptor signaling. *Mol. Brain.* 2011; **4**: 2.
12 Nemoto N, Tsutsui C, Yamaguchi J, Ueno S, Machida M, Kobayashi T, Sakai T. Antagonistic effect of disulfide-rich peptide aptamers selected by cDNA display on interleukin-6-dependent cell proliferation. *Biochem. Biophys. Res. Commun.* 2012; **421**: 129–133.
13 Ueno S, Yoshida S, Mondal A, Nishina K, Koyama M, Sakata I, Miura K, Hayashi Y, Nemoto N, Nishigaki K, Sakai T. *In vitro* selection of a peptide antagonist of growth hormone secretagogue receptor using cDNA display. *Proc. Natl. Acad. Sci. U S A.* 2012; **109**: 11121–11126.
14 Yamaguchi J, Naimuddin M, Biyani M, Sasaki T, Machida M, Kubo T, Funatsu T, Husimi Y, Nemoto N. cDNA display: a novel screening method for functional disulfide-rich peptides by solid-phase synthesis and stabilization of mRNA-protein fusions. *Nucleic Acids Res.* 2009; **37**: e108.

15 Butz K, Denk C, Fitscher B, Crnkovic-Mertens I, Ullmann A, Schröder CH, Hoppe-Seyler F. Peptide aptamers targeting the hepatitis B virus core protein: a new class of molecules with antiviral activity. *Oncogene*. 2001; **20**: 6579–6586.
16 Tomai E, Butz K, Lohrey C, von Weizsäcker F, Zentgraf H, Hoppe-Seyler F. Peptide aptamer-mediated inhibition of target proteins by sequestration into aggresomes. *J. Biol. Chem.* 2006; **281**: 21345–21352.
17 Kurz M, Gu K, Al-Gawari A, Lohse PA. cDNA - protein fusions: covalent protein - gene conjugates for the *in vitro* selection of peptides and proteins. *Chembiochem.* 2001; **2**: 666–672.
18 Tabuchi I, Soramoto S, Nemoto N, Husimi Y. An *in vitro* DNA virus for *in vitro* protein evolution. *FEBS Lett.* 2001; **508**: 309–312.
19 Abdeen SJ, Swett RJ, Feig AL. Peptide inhibitors targeting *Clostridium difficile* toxins A and B. *ACS Chem. Biol.* 2010; **5**: 1097–1103.
20 Gujraty K, Sadacharan S, Frost M, Poon V, Kane RS, Mogridge J. Functional characterization of peptide-based anthrax toxin inhibitors. *Mol. Pharm.* 2005; **2**: 367–372.
21 Ma H, Zhou B, Kim Y, Janda KD. A cyclic peptide-polymer probe for the detection of *Clostridium botulinum* neurotoxin serotype A. *Toxicon.* 2006; **47**: 901–908.
22 Nishikawa K, Watanabe M, Kita E, Igai K, Omata K, Yaffe MB, Natori Y. A multivalent peptide library approach identifies a novel shiga toxin inhibitor that induces aberrant cellular transport of the toxin. *FASEB J.* 2006; **20**: 2597–2599.
23 Sagane Y, Miyata K, Kurihara S, Yoneyama T, Inui K, Miyashita S, Hayashi S, Suzuki T, Niwa K, Watanabe T. Random phage display-based screening of peptides that bind to botulinum neurotoxin binding protein, nontoxic nonhemagglutinin. *Curr. Microbiol.* 2013; **67**: 188–192.
24 Sato A, Ida N, Fukuyama M, Miwa K, Kazami J, Nakamura H. Identification from a phage display library of peptides that bind to toxic shock syndrome toxin-1 and that inhibit its binding to major histocompatibility complex (MHC) class II molecules. *Biochemistry.* 1996; **35**: 10441–10447.
25 Yiadom KP, Muhie S, Yang DC. Peptide inhibitors of botulinum neurotoxin by mRNA display. *Biochem. Biophys. Res. Commun.* 2005; **335**: 1247–1253.
26 Cover TL. The vacuolating cytotoxin of *Helicobacter pylori*. *Mol. Microbiol.* 1996; **20**: 241–246.
27 Tombola F, Carlesso C, Szabò I, de Bernard M, Reyrat JM, Telford JL, Rappuoli R, Montecucco C, Papini E, Zoratti M. *Helicobacter pylori* vacuolating toxin forms anion-selective channels in planar lipid bilayers: possible implications for the mechanism of cellular vacuolation. *Biophys. J.* 1999; **76**: 1401–1409.
28 Ueno S, Nemoto N. cDNA display: rapid stabilization of mRNA display. *Methods Mol. Biol.* 2012; **805**: 113–135.
29 Wada A, Hasegawa M, Wong PF, Shirai E, Shirai N, Tan LJ, Llanes R, Hojo H, Yamasaki E, Ichinose A, Ichinose Y, Senba M. Direct binding of gangliosides to *Helicobacter pylori* vacuolating cytotoxin (VacA) neutralizes its toxin activity. *Glycobiology.* 2010; **20**: 668–678.
30 Chou PY, Fasman GD. Prediction of the secondary structure of proteins from their amino acid sequence. *Adv. Enzymol. Relat. Areas. Mol. Biol.* 1978; **47**: 45–148.
31 Giebel LB, Cass RT, Milligan DL, Young DC, Arze R, Johnson CR. Screening of cyclic peptide phage libraries identifies ligands that bind streptavidin with high affinities. *Biochemistry.* 1995; **34**: 15430–15435.
32 Josephson K, Ricardo A, Szostak JW. mRNA display: from basic principles to macrocycle drug discovery. *Drug Discov. Today.* 2014; **19**: 388–399.
33 Millward SW, Takahashi TT, Roberts RW. A general route for post-translational cyclization of mRNA display libraries. *J. Am. Chem. Soc.* 2005; **127**: 14142–14143.
34 Mochizuki Y, Nemoto N. Evolution of disulfide-rich peptide aptamers using cDNA display. *Methods Mol. Biol.* 2012; **805**: 237–250.
35 Zoller F, Markert A, Barthe P, Hebling U, Altmann A, Lindner T, Mier W, Haberkorn U. A disulfide-constrained miniprotein with striking tumor-binding specificity developed by ribosome display. *Angew. Chem. Int. Ed. Engl.* 2013; **52**: 11760–11764.
36 Yahiro K, Niidome T, Kimura M, Hatakeyama T, Aoyagi H, Kurazono H, Imagawa K, Wada A, Moss J, Hirayama T. Activation of *Helicobacter pylori* VacA toxin by alkaline or acid conditions increases its binding to a 250-kDa receptor protein-tyrosine phosphatase beta. *J. Biol. Chem.* 1999; **274**: 36693–36699.
37 Hansson M, Ringdahl J, Robert A, Power U, Goetsch L, Nguyen TN, Uhlén M, Ståhl S, Nygren PA. An in vitro selected binding protein (affibody) shows conformation-dependent recognition of the respiratory syncytial virus (RSV) G protein. *Immunotechnology.* 1999; **4**: 237–252.
38 Koide A, Bailey CW, Huang X, Koide S. The fibronectin type III domain as a scaffold for novel binding proteins. *J. Mol. Biol.* 1998; **284**: 1141–1151.
39 Binz HK, Amstutz P, Kohl A, Stumpp MT, Briand C, Forrer P, Grütter MG, Plückthun A. High-affinity binders selected from designed ankyrin repeat protein libraries. *Nat. Biotechnol.* 2004; **22**: 575–582.
40 Binz HK, Stumpp MT, Forrer P, Amstutz P, Plückthun A. Designing repeat proteins: well-expressed, soluble and stable proteins from combinatorial libraries of consensus ankyrin repeat proteins. *J. Mol. Biol.* 2003; **332**: 489–503.
41 Pack CG, Aoki K, Taguchi H, Yoshida M, Kinjo M, Tamura M. Effect of electrostatic interactions on the binding of charged substrate to GroEL studied by highly sensitive fluorescence correlation spectroscopy. *Biochem. Biophys. Res. Commun.* 2000; **267**: 300–304.

